Electronic Supplementary Material (ESI) for RSC Advances.

Supporting Information

A Conformationally Persistent Pseudo-bicyclic Guanidinium for Anion Coordination As Stabilized by Dual Intramolecular Hydrogen Bonds

Charles A. Seipp, Neil J. Williams, Vyacheslav S. Bryantsev, Radu Custelcean, and Bruce A. Moyer*

Table of Contents

1. General Information:

^{1}H and ^{13}C spectra were recorded on a Bruker III Advance 400 NMR using DMSO-d6 as solvent. Chemical shifts (δ) are given in ppm and are referenced to residual DMSO in the sample tube. Coupling constants (*J*) are reported in Hz and are classified as singlet (s), doublet (d), triplet (t), broad (br), or multiplet (m). All FT-IR spectra were collected neat on a diamond-ATR equipped Digilab FTS 7000 spectrometer. HR-MS were obtained from an Agilent 6530 qToF using electrospray ionization and the detector set to positive mode.

All reagents and solvents were used as received unless otherwise noted; exceptions to this statement are listed where applicable.

2. General Experimental Procedures:

2.1: Preparation of *N,N'*-bis(2-pyridyl)guanidine (1):

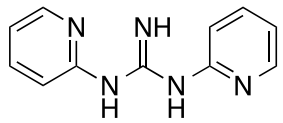

1 was prepared via the method of Toptschiew.[i] *N,N'*-Bis(2-pyridyl)thiourea (2 g, 8.7 mmol), basic lead carbonate (15.0 g, 19.3 mmol), and 7 M ammonia in methanol (7.6 mL, 53 mmol) were added to a sealed tube in 15 mL of ethanol and heated to 45 °C overnight. The flask was cooled, and the black lead salt was filtered off through celite. The solvent was removed *in vacuo* and recrystallized from 10 mL of ethanol to give **1** in 43% yield.

2.2: Preparation of *N,N'*-bis(2-pyridyl)guanidine HCl (2):

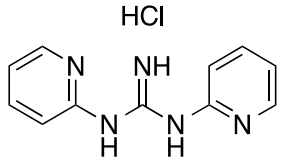

Upon isolation, (**1**) was dissolved into the minimal amount of diethyl ether required to completely solubilize it. At this point, 0.95 equivalents of 1 M HCl in diethyl ether were added while stirring, and the solution allowed to sit for two hours. The precipitate was filtered, rinsed with excess diethyl ether, and isolated as pure **2.**

2.3: Preparation of *N,N'*-bis(2-pyridyl)guanidine hemisulfate (3):

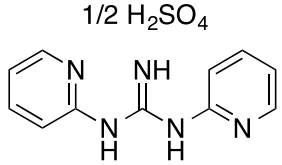

2 was dissolved in the minimal amount of water required to effect complete dissolution. 0.50 equivalents of sodium sulfate dissolved in water (33 mM) were added. The solution was allowed to sit for 60 minutes and then sonicated for 30 minutes. The precipitate was filtered, washed with a small amount of cold water, and dried under vacuum.

2.4: Determination of the Solubility of *N,N'*-bis(2-pyridyl)guanidine hemisulfate Complex:

19.0 mg of **3** was dissolved in 4 mL of millipore-filtered water and allowed to stir for three days at 20 °C as measured by thermometer to fully equilibrate. The residual solid was filtered, and the residual solution was allowed to fully dry in a tared vial to give 10 mg of residual solid. Solubility was thus calculated at 2.5 mg/mL of water.

Carbonate (Na_2CO_3) and phosphate (K_2PO_4) were also checked for complex insolubility. Both anions induced the deprotonation of **1-Cl**, followed by precipitation of the free guanidine.

3. Compound Characterization Data:

3.1: Characterization of *N,N'*-bis(2-pyridyl)guanidine hydrochloride 2:

^{1}H NMR (400 MHz, DMSO-*d6*) δ 10.21 (N-H, 1H, br), 10.20 (N-H, 1H, br), 8.43 (C-H, 1H, d, *J* = 4.8 Hz), 7.97 (C-H, 1H, t, *J* = 7.6), 7.29 (C-H, 1H, t, *J* = 6), 7.21 (C-H, 1H, d, *J* = 8.4) **^{13}C NMR** (100 MHz, DMSO-*d6*) δ 152.97, 151.95, 147.27, 120.53, 114.35. **HRMS:** $C_{11}H_{12}ClN_5$ (Calculated: 214.101, Observed: 214.10550), $C_{22}H_{24}ClN_{10}$ (Calculated: 463.186 Observed: 463.18520) **Melting Point:** 195-197 °C. **IR (Diamond ATR):** 3426 br. w., 3181 br. w., 1690 sh. med., 1497 sh. str., 1468 sh. str., 1359 br. med., 1237 sh. med. 1150 sh. med., 769 sh. str., 697 sh. med., 671 sh. med.

3.2: Characterization of *N,N'*-bis(2-pyridyl)guanidine hemisulfate 3:

^{1}H NMR (400 MHz, DMSO-*d6*) δ 10.49 (N-H, 1H, br), 10.51 (N-H, 1H, br), 8.10 (C-H, 1H, dd), 7.80 (C-H, 1H, dt), 7.19 (C-H, 1H, d, *J* = 8.4), 7.13 (C-H, 1H, dt). **^{13}C NMR** (100 MHz, DMSO-*d6*) δ 154.42, 152.97, 146.89, 139.69, 119.43, 114.93. **HRMS:** $C_{11}H_{12}ClN_5$ (Calculated: 214.101, Observed: 214.10520), $C_{22}H_{24}N_{10}SO_4$ (Calculated: 525.17750, Observed: 525.17560) **Melting Point:** 239-241 °C. **IR (Diamond ATR):** 3312 br. med., 3162 sh. m., 2815 br. w., 1657 sh. str., 1568 sh. med., 1067 sh. str., 742 sh. w., 679 br. med.

3.2.1: Powder Diffraction Pattern of *N,N'*-bis(2-pyridyl)guanidine hemisulfate:

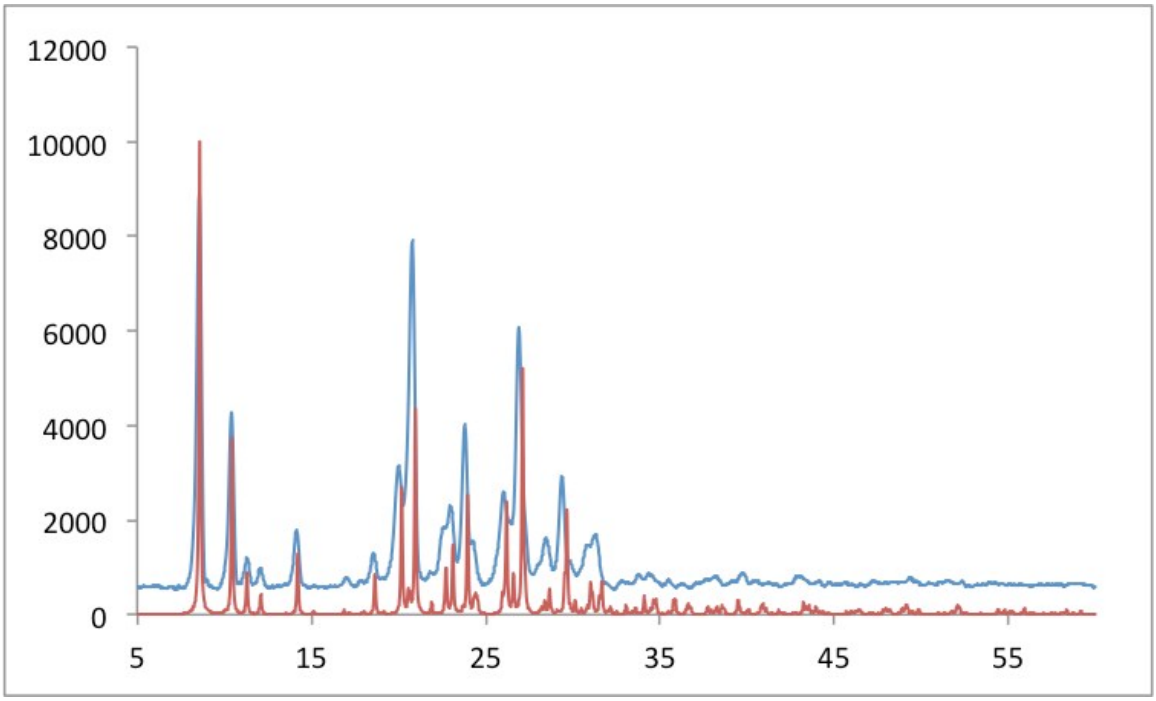

Powder diffraction pattern demonstrating that the bulk precipitate obtained from water has the same structure as the hemisulfate single crystal obtained from pure water. The blue line represents the experimental powder pattern of the bulk precipitate while the red line is the calculated pattern from the single-crystal X-ray data.

4. Computational Details:

4.1: General Computational Information:

Electronic structure calculations were carried out using the Gaussian 09 Revision D.01 software package.[1] The second-order Møller-Plesset perturbation theory (MP2)[2] and three density functional theory (DFT) methods were employed to compare the stabilities of various conformers with different interaction character.

The aug-cc-pVDZ basis set was employed with MP2 calculations, the 6-311++G(d,p) basis set was employed with B3LYP[3] and M06-2X[4] calculations, and the 6-311++G(3df,3pd) basis set was employed with ωB97X-D[5] calculations. The vibrational frequencies of each species were computed at the the B3LYP/6-311++G(d,p) level. The standard enthalpy in the gas phase was computed using the rigid rotor-harmonic oscillator approximation without scaling.

To investigate the sensitivity of calculations to the level of theory and the flavor of the density functional, the comparison of the MP2 and three DFT methods (B3LYP, M06-2X, and ωB97X-D) in predicting relative conformation energies and binding enthalpies is provided in Tables S1 and S2 of Supporting Information. While B3LYP without dispersion correction is known to strongly underestimate the interaction energies of the dispersion-bonded complexes, MP2 is known to seriously overestimate the π-π stacking interaction.[6] The ωB97X-D function is expected to give the most optimal performance, because it gives relative conformation energies intermediate between B3LYP and MP2. This is consistent with the documented ability of the ωB97X-D functional in conjunction with relatively large basis sets to give accurate predictions of binding energies in noncovalent complexes. Based on a superior performance, the results obtained with the ωB97X-D functional were reported in the main text of the manuscript. Natural Bond Orbital (NBO)[7,8] analysis was performed at the ωB97X-D/6-311++G(d,p)//ωB97X-D/6-311++G(3df,3pd) level using NBO version 3 code in Gaussian.[1]

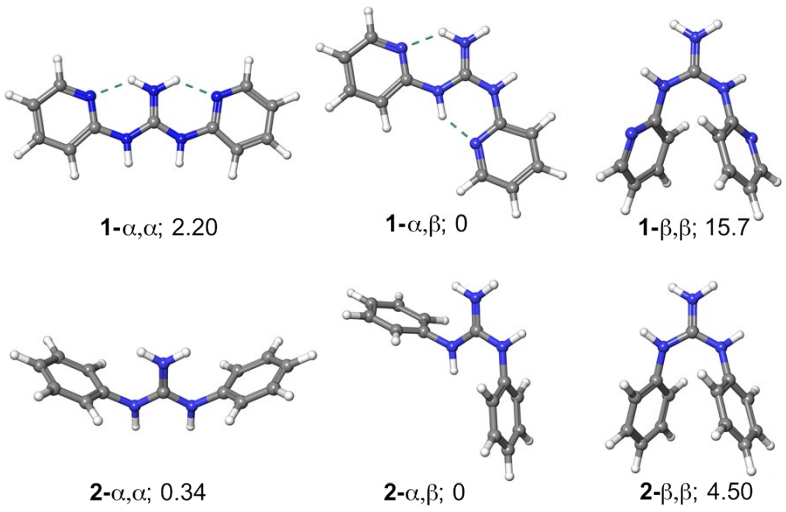

Figure S1. The three major conformations and relative stabilities (ΔH values in kcal/mol) obtained after geometry optimization at the ωB97X-D/6-311++G(3df,3pd) level of theory. Dashed lines indicate hydrogen bonds.

Table S1. Comparison of the MP2 and three DFT methods in predicting relative stabilities of the three major conformations of **1** and **2** (kcal/mol)

Method	Ligand **1**			Ligand **2**		
	α,α	α,β	β,β	α,α	α,β	β,β
MP2/aug-cc-pVDZ	2.72	0	10.4	0.68	0	0.41
B3LYP/6-311++G(d,p)	2.10	0	19.2	0	0.01	6.54
M06-2X/6-311++G(d,p)	1.73	0	14.9	0.02	0	4.63
ωB97X-D/6-311++G(3df,3pd)	2.20	0	15.7	0.34	0	4.50

Conformations are defined in Figure 1. Relative energies are obtained at the ωB97X-D/6-311++G(3df,3pd) level. Zero point energies and thermal corrections to enthalpy are included at the B3LYP/6-311++G(d,p) level.

Table S2. Comparison of the MP2 and three DFT methods in predicting binding enthalpies for 1:1 nitrate anion–ligand complexes in the α,α and α,β binding conformations (kcal/mol)

Method	Ligand **1**		Ligand **2**	
	α,α	α,β	α,α	α,β
MP2/aug-cc-pVDZ	-109.2	-104.7	-105.5	-104.1
B3LYP/6-311++G(d,p)	-102.1	-98.61	-98.22	-97.63
M06-2X/6-311++G(d,p)	-106.5	-102.1	-101.9	-100.9
ωB97X-D/6-311++G(3df,3pd)	-105.7	-102.0	-101.8	-101.0

Binding energies are obtained with respect to a free ligand in the most stable α,β conformation.

Table S3. Second-order stabilization energies (kcal/mol) for the leading donor-acceptor intercations in hydrogen-bonded systems corresponding to a two-electron intermolecular interaction between the NBO lone pair of the Lewis base (n_N or n_O) and the NBO unfilled hydride antibonding orbital of the Lewis acid ($\sigma_{HN(H)}$* or $\sigma_{HN(Pyr)}$*).

Ligand/Complex	$n_N \rightarrow \sigma_{HN(H)}$*	$n_N \rightarrow \sigma_{HN(Pyr)}$*	$n_O \rightarrow \sigma_{HN(H)}$*	$n_O \rightarrow \sigma_{HN(Pyr)}$*
1-α,α	16.9			
1-α,β	19.7	26.2		
1-α,α·NO_3^-	14.8(x2)[a]			41.2(x2)[a]
1-α,β·NO_3^-	11.4	25.6	33.8	48.0

[a]Two equivalent hydrogen bonds.

References for Section 4.1

1. Gaussian 09, Revision D.01, M. J. Frisch, G. W. Trucks, H. B. Schlegel, G. E. Scuseria, M. A. Robb, J. R. Cheeseman, G. Scalmani, V. Barone, B. Mennucci, G. A. Petersson, H. Nakatsuji, M. Caricato, X. Li, H. P. Hratchian, A. F. Izmaylov, J. Bloino, G. Zheng, J. L. Sonnenberg, M. Hada, M. Ehara, K. Toyota, R. Fukuda, J. Hasegawa, M. Ishida, T. Nakajima, Y. Honda, O. Kitao, H. Nakai, T. Vreven, J. A. Montgomery, Jr., J.

E. Peralta, F. Ogliaro, M. Bearpark, J. J. Heyd, E. Brothers, K. N. Kudin, V. N. Staroverov, R. Kobayashi, J. Normand, K. Raghavachari, A. Rendell, J. C. Burant, S. S. Iyengar, J. Tomasi, M. Cossi, N. Rega, J. M. Millam, M. Klene, J. E. Knox, J. B. Cross, V. Bakken, C. Adamo, J. Jaramillo, R. Gomperts, R. E. Stratmann, O. Yazyev, A. J. Austin, R. Cammi, C. Pomelli, J. W. Ochterski, R. L. Martin, K. Morokuma, V. G. Zakrzewski, G. A. Voth, P. Salvador, J. J. Dannenberg, S. Dapprich, A. D. Daniels, Ö. Farkas, J. B. Foresman, J. V. Ortiz, J. Cioslowski, and D. J. Fox, Gaussian, Inc., Wallingford CT, 2009.
2. (a) C. Møller, M. S. Plesset, *Phys. Rev.* 1934, **46** 618-622. (b) M. Head-Gordon, J. A. Pople, M. J. Frisch, *Chem. Phys. Lett.,* 1988, **153**, 503-506.
3. (a) A. D. Becke, *Chem. Phys.,* 1993, **98**, 5648-5652. (b)C. Lee, W. Yang, R. G. Parr, *Phys. Rev. B,* 1988, **37**, 785-789.
4. Zhao, Y.; Truhlar, D. G. *Theor. Chem. Acc.,* **2008**, **120**, 215-241.
5. Chai, J.-D.; Head-Gordon, M. *Phys. Chem. Chem. Phys.,* **2008**, **10**, 6615-6620.
6. K. E. Riley, M. Pitonak, P. Jurecka, P. Hobza, *Chem. Rev.* 2010, **110**, 5023-5063.
7. F. Weinhold and C. Landis, *Valency and Bonding*, Cambridge University Press, Cambridge, 2005.
8. A. E. Reed, L. A. Curtiss, F. Weinhold, *Chem. Rev.,* 1988, **88**, 899-926.

4.2: Additional Computational Insight Into the Selective Crystallization of Sulfate:

To get additional insights into the interaction between guanidinium ligands and SO_4^{2-}, we used density functional theory in its ωB97X-D variant to optimize the geometry for 2:1 complexes of **1** and **2** with $SO_4^{2-}(H_2O)_4$ based on the structural model provided by the **1**-$SO_4^{2-}(H_2O)_4$-**1** crystal structure. Using the crystal structure as the initial configuration, we find that geometry optimization of **1**-$SO_4^{2-}(H_2O)_4$-**1** in the gas phase leads to the S_4 point group symmetry structure. The resulting structure is not drastically different from the initial configuration in which sulfate is fully coordinated via four hydrogen bonds from two guanidinium groups and eight hydrogen bonds from four water molecules. Hessian analysis confirmed this structure to be a true minimum with all positive eigenvalues. Conversely, optimization of **2**-$SO_4^{2-}(H_2O)_4$-**2** in the anti-edge and syn-edge binding configuration and imposing the S_4 and C_2 symmetry, respectively gives rise to geometry exhibiting several imaginary frequencies (Figure S2). Analysis of imaginary modes indicates breaking the S_4 symmetry in the anti-edge configuration by converting to the syn-edge configuration and breaking the C_2 symmetry in the syn-edge configuration by displacing the two water molecules away from the symmetry axis. Thus, the nonplanarity of **2** causes 2:1 complexes with sulfate to have C_1 point group symmetry. The ability of **1** to form high symmetry complexes with sulfate and the overall stronger binding compared to **2** are considered to be the contributing factors leading to the selective crystallization of sulfate with **1** from aqueous solutions.

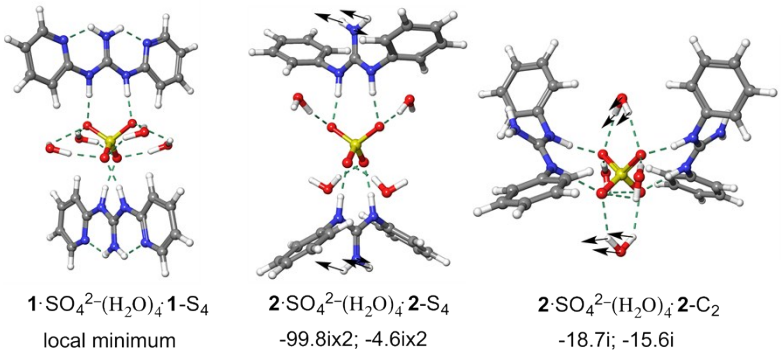

Figure S2. ωB97X-D/6-31+G(d) optimized geometry of 1-$SO_4^{2-}(H_2O)_4$-1 (S_4 point group symmetry) starting from the X-ray crystal structure. Substituting **1** by **2** either in the anti-edge or syn-edge conformation and imposing the S_4 and C_2 symmetry, respectively during optimization gives rise to geometry exhibiting several imaginary frequencies. Arrows show the largest force vectors for imaginary modes. Dashed lines indicate hydrogen bonds.

5. NMR Spectra:

5.1: NMR Spectra of *N,N'*-bis(2-pyridyl)guanidine HCl:

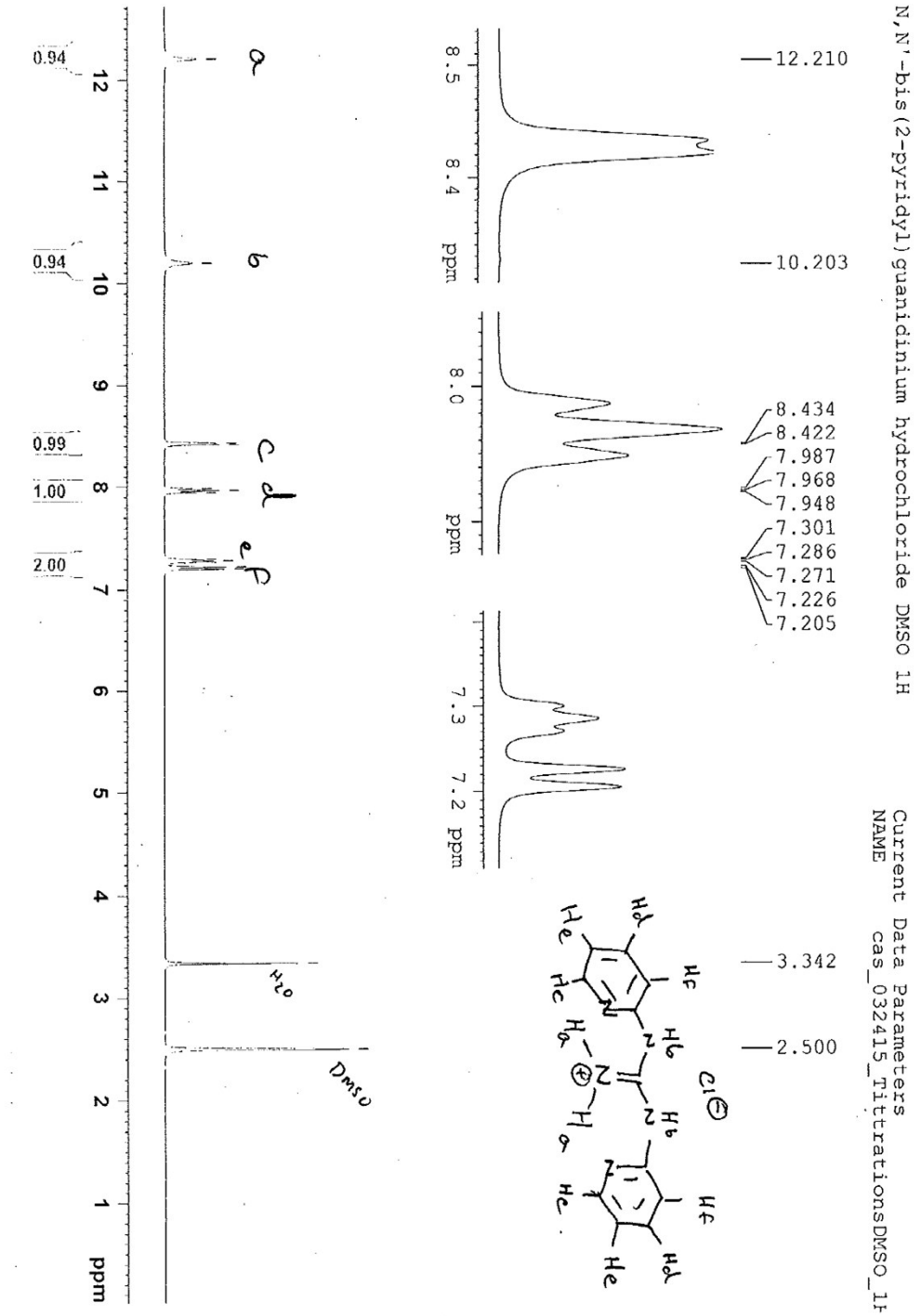

N,N'-bis(2-pyridyl)guanidinium hydrochloride in DMSO-d6 carbon

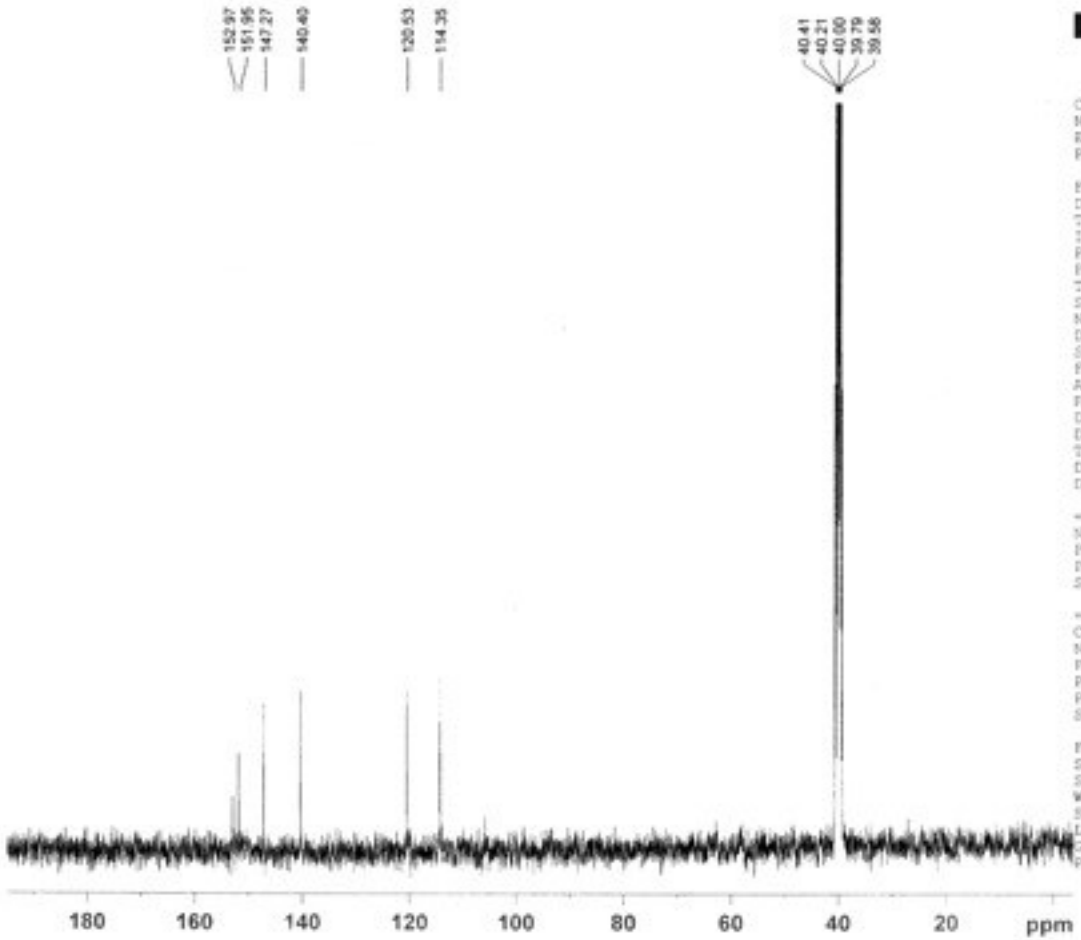

BRUKER

```
Current Data Parameters
NAME      casguanHClCarbon
EXPNO                    2
PROCNO                   1

F2 - Acquisition Parameters
Date_             20150203
Time                 16.18
INSTRUM              spect
PROBHD   5 mm PABBI 1H/
PULPROG           zgpg30
TD                 65536
SOLVENT             DMSO
NS                   1028
DS                      2
SWH              24038.461 Hz
FIDRES           0.366798 Hz
AQ               1.3631988 sec
RG                   2050
DW                20.800 usec
DE                 6.50 usec
TE                297.0 K
D1             2.00000000 sec
D11            0.03000000 sec

======== CHANNEL f1 ========
NUC1                  13C
P1                  10.00 usec
PLW1          44.00000000 W
SFO1         100.4655806 MHz

======== CHANNEL f2 ========
CPDPRG2           waltz16
NUC2                  1H
PCPD2               90.00 usec
PLW2           9.50000000 W
PLW12          0.22988001 W
SFO2         400.3016012 MHz

F2 - Processing parameters
SI                   32768
SF           100.4555150 MHz
WDW                     EM
SSB      0
LB                   3.00 Hz
GB       0
PC                   1.40
```

5.2: NMR Spectra of *N,N'*-bis(2-pyridyl)guanidine Hemisulfate:

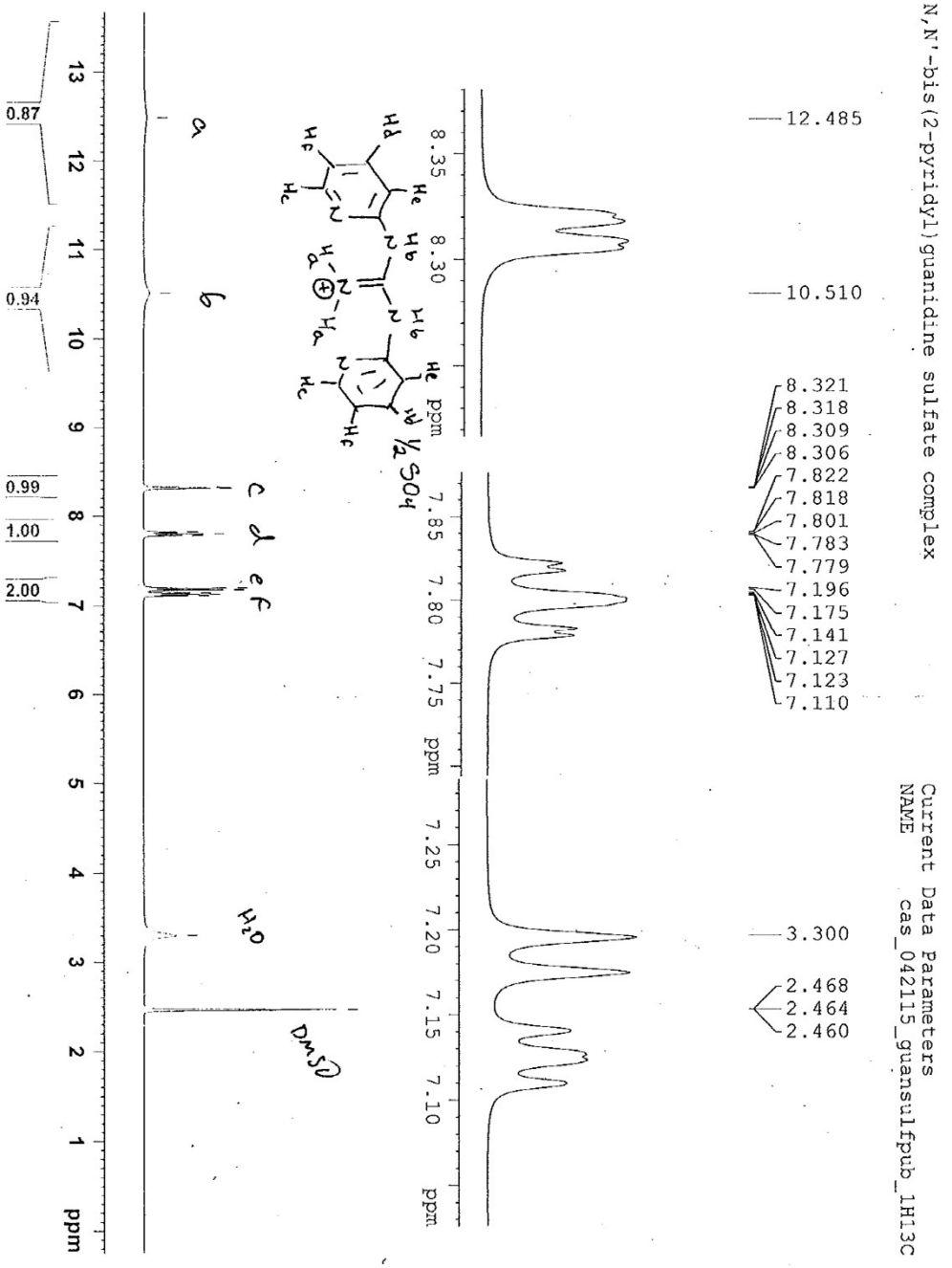

N,N'-bis(2-pyridyl)guanidine hemisulfate

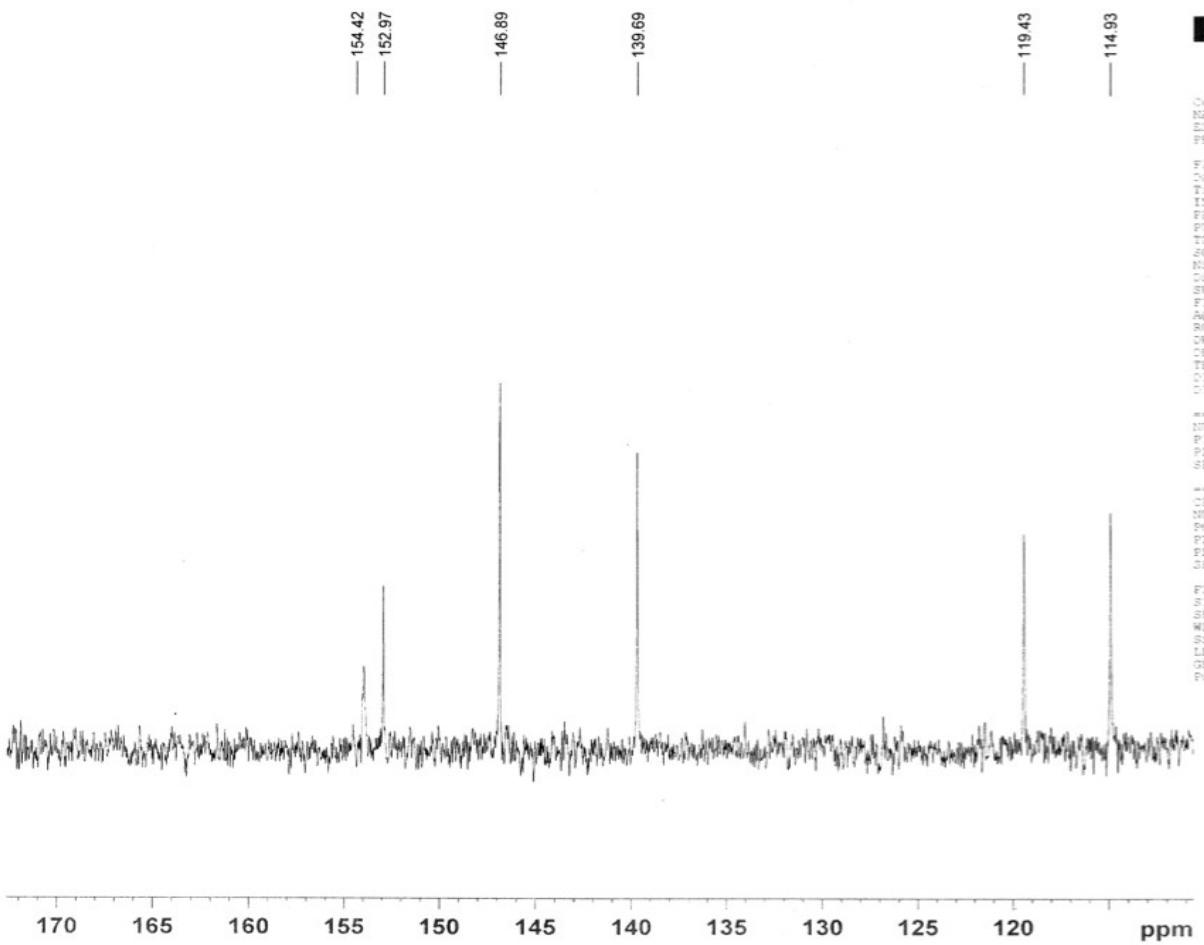

BRUKER

```
Current Data Parameters
NAME      cas_041215_guansulfpub_1H13C
EXPNO                 1
PROCNO                1

F1 - Acquisition Parameters
Date_          20150423
Time              7.00
INSTRUM           spect
PROBHD   5 mm PABBI 1H/
PULPROG          zgpg30
TD               65536
SOLVENT            DMSO
NS                14336
DS                    2
SWH           24038.461 Hz
FIDRES        0.366798 Hz
AQ            1.3631988 sec
RG                 2050
DW               20.800 usec
DE                6.50 usec
TE              296.5 K
D1           2.00000000 sec
D11          0.03000000 sec

======== CHANNEL f1 ========
NUC1               13C
P1               10.00 usec
PLW1         44.00000000 W
SFO1        100.6675937 MHz

======== CHANNEL f2 ========
CPDPRG2          waltz16
NUC2               1H
PCPD2            90.00 usec
PLW2          9.50000000 W
PLW12         0.12983001 W
SFO2        400.3016011 MHz

F2 - Processing parameters
SI                 31766
SF          100.6555150 MHz
WDW                EM
SSB       0
LB                3.00 Hz
GB        0
PC                1.00
```

6. X-ray Crystallography

Single-crystal X-ray data were collected on a Bruker SMART APEX CCD diffractometer with fine-focus Mo Kα radiation (λ = 0.71073 Å), operated at 50 kV and 30 mA. The structures were refined on F^2 using the SHELXTL 6.12 software package (Bruker AXS, Inc., Madison, WI, 1997). Absorption corrections were applied using SADABS. Hydrogen atoms were placed in idealized positions, except for the protons of the water molecules in 1-SO_4 water, which were located from the difference Fourier maps and refined isotropically. CCDC 1404793-1404796 contains the supplementary crystallographic data for this paper. These data can be obtained free of charge from The Cambridge Crystallographic Data Centre via www.ccdc.cam.ac.uk/data_request/cif.

[i] Toptschiew, *Archiv der Pharmazie,* **1934**, vol. 272, p.775-778